Concentration dynamics of nitric oxide in rat hippocampal subregions evoked by stimulation of the NMDA glutamate receptor

Ana Ledo*, Rui M. Barbosa*, Greg A. Gerhardt†, Enrique Cadenas‡, and João Laranjinha*§

*Faculty of Pharmacy and Center for Neurosciences and Cell Biology, University of Coimbra, 3000 Coimbra, Portugal; †Department of Anatomy and Neurobiology, University of Kentucky, Lexington, KY 40506-0098; and ‡Department of Molecular Pharmacology and Toxicology, University of Southern California, Los Angeles, CA 90089-9121

Edited by Salvador Moncada, University of London, London, United Kingdom, and approved October 5, 2005 (received for review May 9, 2005)

Nitric oxide (•NO) production in response to stimulation of the NMDA glutamate receptor is implicated not only in the synaptic plasticity in hippocampus but may also participate in excitotoxic cell death. Using •NO-selective microssensors inserted into the diffusional field of •NO in acute hippocampal slices, we describe the •NO concentration dynamics evoked by NMDA receptor activation and report profound differences along the trisynaptic loop of the hippocampus. We measured the oxygen gradient across the slice thickness and conclude that •NO measurements were performed at cell layers experiencing physiological oxygen tensions. Recordings performed at increasing distances from the point of NMDA receptor stimulation resulted in a progressive decrease of •NO signals, reaching undetectable levels for distances >400 μm, supporting the notion of a wide diffusional spread of endogenously generated •NO in the hippocampus. Neither a picoinjection nor a continuous perfusion of NMDA resulted in high steady-state •NO levels; rather all signals were transient, suggesting that cells are able to efficiently respond to high •NO concentrations (typically 200–400 nM) bringing it to very low nM levels; the claimed high micromolar •NO range achieved by excessive stimulation of NMDA receptor may have to be reevaluated. The distinct responses to NMDA receptor stimulation along the trysynaptic loop suggest a differential •NO activity and/or regulation among the hippocampal subregions. These findings may be relevant for the understanding of the role of •NO in physiologic mechanisms in the hippocampus and the differential sensitivity of the hippocampal subregions to NMDA receptor-dependent neurodegeneration.

carbon fiber microelectrode | NO diffusional spread | hippocampus

A neural role of nitric oxide (•NO) as an intercellular signaling molecule in the nervous system was first suggested by Garthwaite and Boulton (1), who related the activation of glutamate NMDA receptor and •NO synthesis in brain slices. This notion has been confirmed by subsequent studies (for review see ref. 2). Conversely to conventional messenger molecules in the brain, because of its low molecular weight, hydrophobic nature, and very high diffusion constant, •NO diffuses isotropically from its site of synthesis regardless of overruling cellular or membrane structures (3, 4). Thus, the current understanding of •NO bioactivity in the brain implies the formation of a "sphere of influence" of •NO affecting a volume of tissue containing many neurons irrespective of functional connections through synapses; i.e., •NO operates as a diffusible intercellular messenger. A critical tenet of •NO bioactivity establishes that its actions at any location are determined by the local •NO concentration (5). Yet, the evaluation of •NO in terms of concentration dynamics has been limited because of the difficulties in measuring •NO with spatiotemporal resolution and appropriate sensitivity and selectivity. Although it has been shown that •NO produced postsynaptically exerts actions at the presynaptic level (6–9), the quantification of the diffusional spread of endogenously generated •NO in the brain lacks experimental evidence. Theoretical modeling predicted that •NO produced from a single physiologic source for 1–10 s diffuses within a 200-μm-diameter sphere (4).

The hippocampus is a structure of the brain medial temporal lobe implicated in declarative memory formation (10) affected during aging and Alzheimer's disease (11). At glutamatergic synapses in hippocampus (12), the link between NMDA receptor activation and the production of •NO by neuronal NO synthase (nNOS) is Ca^{2+} entry through the activated receptor channel, leading to the formation of the Ca^{2+}/calmodulin complex, which in turn is capable of activating intracellular nNOS (1).

The measurement of •NO dynamics during functionally induced changes in the hippocampus by activation of the NMDA receptor has generated much interest inasmuch as the activation of this receptor is essential to signaling pathways that underlie neuronal plasticity, but also triggers neurodegeneration that occurs in senescence and disease, suggesting a role for •NO in these processes (13). For instance, in the CA1 and dentate gyrus (DG) subregions of the hippocampus, long-term potentiation (LTP) is triggered by the activation of the NMDA receptor as a result of heavy stimulation of the presynaptic terminal (14). In this context, •NO has been suggested to be the diffusible retrograde messenger required for LTP (15, 16).

Excessive activation of the NMDA receptor mediates neurodegeneration in neurological disorders, inducing Alzheimer's disease, Parkinson's disease, multiple sclerosis, and AIDS dementia (13, 17). •NO has been implicated in such excitotoxic phenomenon in a variety of cellular model systems (13, 18).

All of this information leads to the notion of •NO as a crucial mediator of pathophysiological pathways in the hippocampus. Yet, knowledge regarding the concentration dynamics of endogenously produced •NO is scarce and, clearly, this knowledge is imperative in understanding its role in signaling pathways. In this study, we use microssensors developed to monitor the dynamics of •NO production and decay in the different subregions of acute rat hippocampal slices upon stimulation of the NMDA receptor. First, we determined the spread of endogenously generated •NO and, then, inserting the sensors within the diffusional field of •NO, we studied its concentration dynamics and provided evidence for a heterogeneous distribution and transient nature of •NO signals as a function of the hippocampal subregion.

Materials and Methods

Chemicals and Solutions. NMDA, D-(-)-2-amino-5-phosphonopentanoic acid (D-AP5), and N_G-nitro-L-arginine (L-NNA) were ob-

Conflict of interest statement: No conflicts declared.

This paper was submitted directly (Track II) to the PNAS office.

Abbreviations: nNOS, neuronal NO synthase; DG, dentate gyrus; LTP, long-term potentiation; D-AP5, D-(-)-2-amino-5-phosphonopentanoic acid; L-NNA, N_G-nitro-L-arginine; AA, ascorbate; aCSF, artificial cerebrospinal fluid.

§To whom correspondence should be addressed. E-mail: laranjin@ci.uc.pt.

tained from Tocris Cookson (Avonmouth, U.K.). Ascorbate (AA), dopamine, and *o*-phenylenediamine were from Fluka. 5-Hydroxytryptamine, glutathione, diethylenetriaminepentacetic acid, and diethylenetriamine/nitric oxide adduct were from Sigma. Nafion was from Aldrich, and nitrite was from Merck. All other reagents were reagent grade.

Buffer used for microsensor testing and calibrations was PBS with the following composition: 140 mM NaCl, 2.7 mM KCl, 8.1 mM $NaHPO_4$, 1.8 mM KH_2PO_4, and 0.1 mM diethylenetriaminepentacetic acid, pH 7.4.

Media for hippocampal slice experiments were artificial cerebrospinal fluid (aCSF) composed of 124 mM NaCl, 2 mM KCl, 25 mM $NaHCO_3$, 1.25 mM KH_2PO_4, 1.5 mM $CaCl_2$, and 10 mM D-glucose. For dissection and recovery modified aCSF was used to increase viability. Composition of this aCSF was 124 mM NaCl, 2 mM KCl, 25 mM $NaHCO_3$, 1.25 mM KH_2PO_4, 0.5 mM $CaCl_2$, 10 mM $MgSO_4$, 0.2 mM AA, 1 mM glutathione, and 10 mM D-glucose. In both cases, aCSF was continuously bubbled with humidified carbox (95%O_2/5%CO_2) for pH buffering (pH 7.4) and oxygenation.

Electrochemical Instrumentation. Fast cyclic voltammetry was carried out on an EI-400 potentiostat (Ensman Instruments, Bloomington, IN), and signals were monitored on a digital storage oscilloscope (Tektronix TDS 220).

Amperometric currents from microsensor modification and calibration and oxygen measurements in tissue were recorded on a PGSAT 12 potentiostat (EcoChimie, Utrecht, The Netherlands) with low current module, controlled by GPES software, version 4.9. Amperometric currents recordings in slices were performed on the inNO model T electrochemical detection system (Innovative Instruments, Tampa, FL).

In hippocampal recordings of both $^{\bullet}NO$ and O_2, a two-electrode circuit was used, with a Ag/AgCl pellet as a reference electrode and the microsensor as a working electrode. For other experiments, a three-electrode cell with a Pt-wire auxiliary electrode, a Ag/AgCl (3M) reference electrode, and the microsensor as a working electrode was used.

The working electrode was held at a constant potential of either +0.9 or −0.8 V for $^{\bullet}NO$ or O_2 measurements, respectively.

$^{\bullet}NO$ Microsensor Construction and Surface Modification. Microsensors were fabricated as described (19–21). Briefly, single carbon fibers (8 μm i.d.; Courtaulds, London) were inserted into borosilicate glass capillaries (1.16 mm i.d. × 2.0 mm o.d.; Harvard Apparatus), cleaned with acetone, and pulled on a vertical puller (Harvard Apparatus).The protruding carbon fibers were cut to tip length of ≈100 μm. The electrical contact between the carbon fiber and the copper wire was provided by conductive silver paint (RS, Northants, U.K.).

Microsensors were first coated with Nafion by dipping the fiber into a Nafion solution at room temperature for 30 s and drying for 10 min at 170°C in an oven. Microsensors were then modified by electropolimerization of *o*-phenylenediamine (*o*-PD) as described (22). A 5-mM *o*-PD solution in PBS supplemented with 0.1 mM AA was made fresh each day and used immediately. Electropolimerization on the carbon surface was preformed by amperometry at constant potential of +0.9 V vs. Ag/AgCl for 15 min.

Microsensor Testing Procedures. Each microsensor was tested for general recording characteristics in PBS by using fast cyclic voltammetry at a scan rate of 200 V/s between −0.4 and +1.6 V. This potential range provides an electrical pretreatment of the carbon fiber that improves sensitivity. A stable background current and sharp transients at reversal potentials indicated suitable recording properties of the microsensor.

The microsensors for $^{\bullet}NO$ were calibrated by a single stream flow injection analysis system by using a homemade flow cell with PBS as a carrier solution at a flow rate of 2.0 ml/min. Transient oxidation currents were measured in response to 100 μl of diethylenetriamine/NO adduct solution in deaerated PBS injected repeatedly with a four-valve port.

The microelectrodes for O_2 measurement were calibrated in a 2-ml cell with PBS as a support electrolyte. The reduction current was measured for three distinct O_2 tensions (0, 156, and 700 torr) achieved by bubbling the PBS with argon, allowing it to achieve atmospheric PO_2 and bubbling it with Carbox, respectively.

Rat Hippocampal Slices. Male Wistar rats (100–150 g) were killed by cervical displacement according to approved guidelines. The brain was rapidly removed and placed in ice-cold modified aCSF. The hippocampi were dissected and placed on the stage of a McIlwain tissue chopper (Campden Instruments, London), and 400-μm-thick sections were obtained. The slices were separated and transferred to a preincubation chamber (BSC-PC, Harvard Apparatus) containing modified aCSF at room temperature, continuously bubbled with Carbox. Slices were recovered under these conditions for at least 1 h before recordings.

Recording $^{\bullet}NO$ Concentration Dynamics. Individual slices were placed in a recording chamber (BSC-BU with BSC-ZT top, Harvard Apparatus) and perfused with normal aCSF at 32°C (temperature controller model TC-202A, Harvard Apparatus) continuously bubbled with humidified Carbox at a flow rate of 2 ml/min. A microsensor was placed in the desired subregion of the hippocampal slice (for CA1 and CA3 subregions the microsensor was placed at the level of the pyramidal cell layer and in the DG at the granular cell layer) 100–200 μm into the tissue. These sites are known to be concentrated in nNOS (23, 24) and were easy to identify, enabling precise reproduction of microsensor insertion.

For slice stimulation, a pressure ejection protocol was applied, using a Picospritzer II (General Valve, Fairfield, NJ). A glass pipette capillary with an inner tip diameter of 8 μm was filled with stimulation solution (5 mM NMDA in 0.1 M phosphate buffer containing 154 mM NaCl, pH 7.4) and placed at the slice surface ≈50 μm away (or as otherwise indicated) from the point of insertion of the microsensor. A 3-s pulse was applied at a pressure of 10 psi. In experiments where antagonists or inhibitors were used these drugs were added to the perfusion media.

Measurement of PO_2 Across Slice Thickness. The oxygen tension (PO_2) across the hippocampal slice was measured as described (25). Bare carbon fiber microelectrodes were prepared as described above for the $^{\bullet}NO$ microsensor, with no surface modification. The exposed tip was cut at 10–20 μm to increase spatial resolution in recordings.

The microelectrode was placed at different depths (surface, 100, 200, 300, or 400 μm) of the tissue with the help of a micromanipulator.

Data Analysis. Data are expressed as the mean ± SEM and were analyzed for statistical significance defined as $P < 0.05$ using Student's *t* test. Total charge was calculated as the time integral of the amperometric current.

The individual $^{\bullet}NO$ recordings obtained in the different subregions of hippocampal slices challenged with NMDA were divided into two phases: ascendant and descendent. The ascending phase was fitted to a sigmoid function, which allowed the T_{80} for this phase to be calculated. The descending phase was fitted to an exponential first-order decay function and the time constant was calculated for each recording.

All analysis was performed with commercially available software.

Results

Determination of $^{\bullet}NO$ Diffusion Field in Hippocampal Slices. Experiments illustrated in Fig. 1 were aimed at determining the diffusional

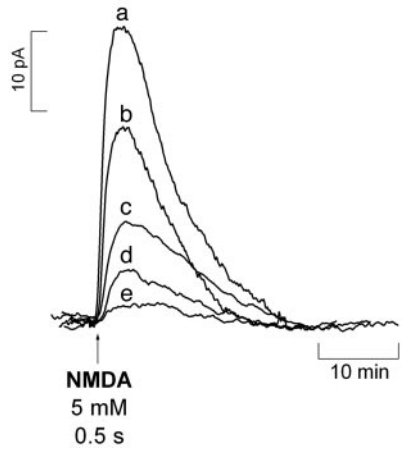

Fig. 1. Diffusional spread of •NO produced upon NMDA receptor activation. The •NO microssensor was inserted in the CA1 pyramidal cell layer, and the stimulation pipette was placed at increasing distances: 0 μm (*a*), 100 μm (*b*), 200 μm (*c*), 300 μm (*d*), and 400 μm (*e*). The stimulus consisted of a 500-ms ejection of NMDA (5 mM).

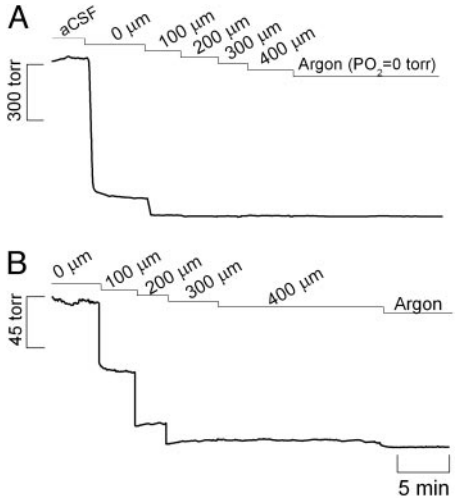

Fig. 2. Oxygen tension (PO_2) along the hippocampal slice depth. (*A*) Demonstrated is the dramatic decrease in PO_2 when the sensor was placed at the surface of the tissue and then at increasing depths into the tissue. (*B*) Shown is the PO_2 gradient within the tissue. Recordings were performed in the CA1 pyramidal cell layer of the hippocampal slice.

field of •NO, after activation of multiple NOSs via NMDA receptor in the CA1 subregion of the hippocampal slice. The •NO sensor was placed at increasing distances from the site of stimulation by ejection of NMDA, namely 0, 100, 200, 300, and 400 μm. The stimulation parameters were selected to guarantee that NMDA diffusion in the tissue was kept <100 μm, which was accomplished by decreasing the ejection time to 500 ms (the NMDA concentration and the ejection pressure were maintained at 5 mM and 10 psi, respectively). This condition was reached by measuring the diffusional field of a 5-mM solution of AA (assumed to have a diffusion in the tissue similar to that of NMDA) in the hippocampal slice by using a bare carbon fiber microelectrode inserted in the tissue.

As shown in Fig. 1, as one draws back from the site of NMDA stimulation, the amplitude of the recorded •NO signal decreases significantly, becoming undetectable >400 μm. It is noteworthy that this experimental figure is in general agreement with published theoretical calculations for •NO diffusion in tissues (3–5, 26).

Determination of Oxygen Gradients in Hippocampal Slices. The reaction of •NO with O_2 is slow under the normoxic conditions of tissues (27), and, although little is known about how •NO is inactivated, the reaction with O_2 in tissues is not likely to be a significant contributing route for •NO decay. However, at variance with the physiological environment, the reaction of •NO with O_2 may acquire significance for the high oxygen tensions used in the perfusion experimental system, thus misleading •NO dynamics by enhancing the rate of •NO decay. Therefore, we measured the tension of O_2 across slice thickness. The results shown in Fig. 2*A* indicate a steep gradient of oxygen decreasing from the surface to the inner cell layers. At 200 μm deep (Fig. 2*B*) the tension of O_2 is $\approx 6 \pm 1$ torr ($n = 8$), which, considering that the reported O_2 tension in the CNS of rat is 10–30 torr (28–30), indicates that at the core of the tissue slice the measured •NO dynamics are not erroneously affected by a nonphysiological O_2 tension.

Dynamics of •NO Concentration in the Different Subregions of the Rat Hippocampal Slices. To study the concentration dynamics of •NO in the distinct subregions of the hippocampal slice, NMDA (5 mM solution) was ejected at the surface of the tissue, on top of the microssensor insertion point and for a period of 3 s, to guarantee maximal receptor activation. Typical recordings obtained in the *stratum pyramidale* of subregions CA1 and CA3 and the *stratum granulosum* of the DG subregion are shown in Fig. 3*A*.

Values of T_{80} of the ascending phase and the decay constants of the descending phase of •NO signals in the different subregions are indicated in Table 1. Regarding the kinetics of •NO increase, no significant difference ($P < 0.05$) was seen when comparing CA1 and CA3 subregions. However, T_{80} was significantly ($P > 0.05$) longer for DG, as compared with the other subregions, reflecting a much slower production of •NO. No significant differences were observed in the decay phase ($P < 0.05$).

The charge produced during the oxidation of •NO at the sensor active surface (which is linearly proportional to •NO concentration) was calculated for the different subregions (Fig. 3*B*). Among all regions, the CA1 showed the largest production of •NO upon stimulation with NMDA. For the experimental conditions selected, a typical peak of •NO in CA1 subregion was 300 ± 80 nM ($n = 41$) but in the other subregions average •NO levels reached 50 nM.

Blocking the NMDA Receptor with D-AP5. To confirm that •NO production was a result of the specific activation of NMDA receptor, the effect of the NMDA receptor antagonist D-AP5 was examined on NMDA-induced signals measured in the CA1 subregion (because responses to NMDA receptor activation were both more robust and reproducible in this subregion). Fig. 4 shows the effect of D-AP5 added to the perfusion media after a typical response was obtained for a standard stimulation. After 20 min of perfusion with D-AP5, the slice was stimulated for a second time. The NMDA receptor antagonist was then washed out for 20 min before the slice was again stimulated with NMDA. As illustrated in Fig. 4, D-AP5 substantially decreased •NO production and, after its removal from the perfusion medium, the response increased to the values typically obtained for a second stimulation. In the CA1 subregion, the average decay in amplitude of signal from the first to second stimulation was $44.9 \pm 6\%$ ($n = 28$, data not shown) and $4.0 \pm 1.7\%$ ($n = 3$) in the absence and presence of D-AP5 during the second stimulation, respectively.

Inhibition of NOS. The NOS inhibitor L-NNA was used to verify that the enzyme was responsible for observed signals evoked by activation of the NMDA receptor. Fig. 5 shows a typical recording in the CA1 subregion of the hippocampus documenting the effect of L-NNA (a competitive inhibitor of NOS) added to the perfusion medium after an initial response to NMDA. Treatment with 200 μM L-NNA inhibited •NO production upon a second stimulation with NMDA. After a first stimulation, the signals subsequent to the

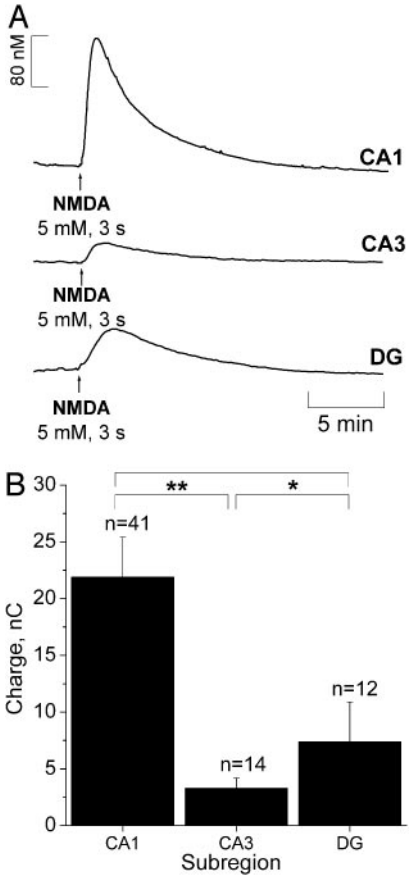

Fig. 3. NMDA-evoked •NO production in hippocampus. (*A*) Typical current recordings in distinct subregions of the rat hippocampal slice. In the CA1 and CA3 subregions recordings were performed in the pyramidal cell layer, and in the DG they were performed in the granular cell layer. (*B*) Average charge was measured in each subregion upon NMDA receptor activation. Statistical analysis of the differences were assessed by Student's *t* test (*, $P > 0.05$; **, $P < 0.05$).

second stimulation are 44.9 ± 6.0% ($n = 28$) and 8.8 ± 4.3% ($n = 3$) in the absence and presence of L-NNA, respectively.

Continuous Stimulation of the NMDA Receptor. Because brief stimulation in the CA1 subregion by pressure ejection resulted in a transient increase in •NO concentration, the question arose as to whether prolonged exposure to NMDA could lead to a steady-state rise in the free radical concentration. Fig. 6 shows that even when the tissue was continuously perfused with 10 μM NMDA •NO production was transient (Fig. 6*A*), although more robust than in the case of brief stimulation. Also, when the competitive NMDA receptor antagonist D-AP5 was added during the decay phase of the signal (Fig. 6*B*), decay rate increased, but not abruptly, indicating that the active receptor was still functionally coupled to •NO production.

Table 1. The T_{80} for sigmoidal increase and time constant of the decay calculated from NMDA-induced •NO signals in different subregions of the rat hippocampal slice

	Parameters	
Subregion	T_{80} (s) ± SEM	Time constant (s) ± SEM
CA1	45 ± 8	247 ± 16
CA3	43 ± 9	174 ± 74
DG	141 ± 34	211 ± 30

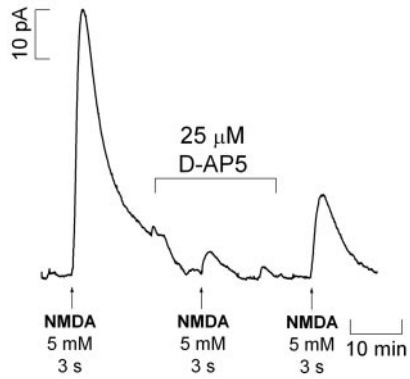

Fig. 4. Typical recording of oxidation currents in the CA1 pyramidal cell layer of the hippocampal slice with and without D-AP5, a competitive inhibitor of NMDA receptors.

Discussion

The activity of •NO as an intercellular signaling molecule in the brain has been generally established with experimental models using •NO donors, inhibitors of •NOS, and the so-called "•NO scavengers," or, alternatively, in experimental models that do not involve the measurement of endogenously produced •NO, but use indirect measurements that require sample processing and lack spatiotemporal resolution (2, 31, 32).

This work provides evidence for heterogeneous •NO concentration dynamics in the hippocampal sugregions, functionally dependent on the stimulation of the NMDA subtype of glutamate receptor (Fig. 3). Considering the evanescent nature of •NO as a diffusible messenger in the hippocampus, its measurement with an electrochemical microsensor inserted in the •NO diffusional field, experimentally determined in our system, provided the appropriate spatial resolution. Further critical features of the measurements performed include real-time analysis, sensitivity in the low nM range, and high selectivity against interfering substances potentially present at high concentrations such as indols, catechols, and AA (20). The inhibition of the •NO signal by a NOS inhibitor (Fig. 5) strongly supports the selective measurement of •NO. Instrumental controls (see Figs. 7 and 8, which are published as supporting information on the PNAS web site) involving amperometry at +0.9 vs. +0.4 V and differential pulse amperometry further contributed to support the selectivity of measurements performed. Briefly, a comparison between the total charge produced in the CA1 subre-

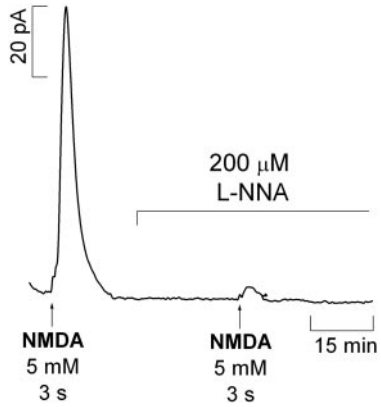

Fig. 5. Typical recording of the effect of L-NNA (200 μM), a competitive inhibitor of NOS, in •NO signals evoked by pressure ejection of NMDA (5 mM) for 3 s in the CA1 pyramidal cell layer. The inhibitor was added to the perfusion media after a positive response to a first stimulation was obtained.

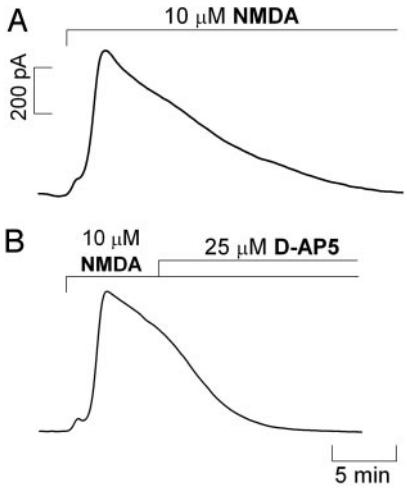

Fig. 6. •NO production evoked by continuous perfusion of 10 μM NMDA. Recordings were performed in the CA1 pyramidal cell layer of rat brain slices. (*A*) A continuous stimulation with NMDA. (*B*) A continuous stimulation with addition of 25 μM D-AP5 during the decay of the signal. Typical recording is representative of several done.

gion for the two working potentials, +0.9 and +0.4 V, shows that at +0.9 V total charge of recorded signals was 23 +/− 4 nC (n = 35) and at +0.4 V total charge was 1.1 +/− 0.6 nC (n = 7). Moreover, a differencial pulse amperometry recording in the CA1 subregion followed similar kinetics to the amperometric recordings and 10 μM of dopamine, 5-hydroxytryptamine, and AA were not significantly detected, as would be expected because only electroactive species oxidized between +0.7 and +0.9 V are detected. Finally, •NO dynamics were measured in the cell layers experiencing an O_2 tension similar to that found *in vivo* (Fig. 2), thus excluding a reaction with O_2 as a major route for •NO decay.

There are a number of possible cellular sources for constitutive NOS activity in the hippocampus, including nNOS from neurons and interneurons, endothelial NOS from endothelial cells in blood vessels (33–38), and constitutive NOS activity deriving from astrocytes (39). The use of NMDA as the test stimuli imparts specificity to the production of •NO via the NMDA glutamate receptor-nNOS pathway.

Specifically, the major findings can be listed as follows: (*i*) the diffusional field of •NO upon stimulation of multiple NOSs within a radius of 100 μm is ≈400 microns in the CA1 subregion; (*ii*) •NO signals are transient even under conditions of continuous stimulation of the NMDA receptor; (*iii*) •NO is produced in all subregions in response to NMDA receptor stimulation; (*iv*) •NO concentration dynamics (rate and pattern of production and decay) is heterogeneous along the trisynaptic loop in the cell body layers of the CA1, CA3, and DG subregions; (*v*) a steep gradient of O_2 is operative in the slice cell layers, being physiological at the core of the tissue; (*vi*) cells efficiently bring •NO to low nM levels, preventing high steady concentrations; and (*vii*) at variance with current dogma, the NMDA receptor does not suffer a feedback blockage by •NO.

Experimental evidence and theoretical models for •NO diffusion in biological settings support the notion that •NO is highly diffusible (diffusing more rapidly than it reacts) and spreads randomly in all directions driven by a spatial concentration gradient from its local of synthesis (3–5, 26, 40, 41). In addition to its diffusibility, the amount and rate at which it is generated, the duration of release from a source cell, and the type and number of targets in the vicinity as well as the rate (and compartmentalization) of chemical reactions shape the •NO concentration-time profile. The experimental approach used in this study implies that multiple •NO sources within a tissue volume are simultaneously activated by the localized ejection of NMDA. Under these conditions, encompassing the diffusion of NMDA in the tissue and a perfusion flow of 2 ml/min, •NO diffused at least >400 microns from the NMDA ejection site. Of note, within this tissue volume, •NO signals are transient. The transitory nature of •NO signals was also observed under conditions where the slices were continuously perfused with NMDA (Fig. 6*A*). However, in this case, the decay was linear and slower compared with the ejection approach, which is characterized by an exponential decay (e.g., Fig. 3*A*), and D-AP5 brings •NO to basal levels, thus suggesting that NMDA receptor-dependent •NO synthesis is operative (Fig. 6*B*). The perfusion system is unlikely to determine the transitory nature of the signals as perfusion of a 400 nM solution of •NO prepared from •NO gas induced a constant signal (data not shown). These observations suggest that, at variance with what is conventionally expected, maintaining a continuous and simultaneous activation of multiple cellular •NO sources does not result in a monotonous rise of •NO or high steady-state concentrations, rather the concentration of •NO rises transiently. The decay of •NO observed under continuous perfusion is not likely to be accounted for by a negative feedback of NOS (42, 43) or the NMDA receptor, known to occur through S-nitrosylation of specific SH residues (44–49), for D-AP5 would have induced no inhibition of •NO decay kinetics. Thus, the results suggest the occurrence of mechanisms for the prevention of high steady-state •NO concentrations. In agreement with this notion, it has been recently proposed that brain cells possess powerful •NO inactivation mechanisms that shape •NO signals (50, 51). At variance with the synthesis of •NO by NOS, which is a highly regulated process (52), its decay/consumption is thought to be an unregulated process, depending largely on the local availability of potential targets (hemoglobin, soluble guanylate cyclase, cytochrome oxidase, superoxide anion, thiol groups. . .). The results shown here are consistent with the view whereby brain cells are able to efficiently respond to a high •NO concentration bringing it to very low nM levels.

The subregional differences in •NO signals evoked with NMDA raise at least two important questions: what are the underlying mechanisms and how do these differences translate into tissue physiological activity?

Regarding the latter, it may be noted that the strength of •NO responses in CA1 pyramidal neurons accomplishes an essential requirement posed by the notion of •NO as a messenger in synaptic plasticity mechanisms linked to memory and learning: NMDA-dependent LTP (53) is seen mainly in the CA1 subregion of the hippocampus; in CA3 a different type of potentiation is observed (54). Moreover, in humans, a regional-specific neuron loss in CA1 region is associated with the cognitive decline in Alzheimer's disease (55). Thus, one might expect to see differences in •NO concentration dynamics in CA1 relative to CA3 and DG.

The elucidation of the mechanisms that support the subregional differences of •NO signals is an open question. It is currently conceived that the neuronal isofoform of NOS is not confined to small specific areas, but is distributed in a small population of neurons throughout brain areas, including hippocampus (36). Assuming a homogeneous distribution of nNOS and NMDA receptor, the heterogeneous concentration dynamics of •NO among the subregions of hippocampus evoked by stimulation of NMDA receptors suggests a region–specific regulation of •NO bioactivity. However, despite species and development variations in hippocampal nNOS (37), there may also be a gradient of expression of nNOS in the subregions of the hippocampus. A recent report showed a higher level of nNOS expression in the CA1 subregion of the rat hippocampus, but these observations were made in the total extract of each region in a manner that cannot distinguish between nNOS that is coupled to the NMDA receptor and nNOS present in other cellular compartments (38). Also, the differences reported are not as large as the ones shown in this study for •NO production.

It may be argued that the differential level of expression of the NMDA receptor in the subregions of the hippocampus may account for the differential NMDA-dependent •NO signals observed.

This type of glutamate receptor is more highly expressed in the CA1 subregion (56). In agreement with this hypothesis, reports on the production of $^{\bullet}$NO in hippocampal subregions not dependent on NMDA receptors showed less significant differences of $^{\bullet}$NO production as compared with those in this study. Smith *et al.* (57), using nicotine as the stimulus for $^{\bullet}$NO production, reported that CA3 and DG peak amplitudes were ≈70% of peak amplitude in CA1 area. More recently, a bioimaging approach with diaminofluorescein derivatives indicated that $^{\bullet}$NO is produced mainly in the CA1 area in hippocampal slices under ischemic conditions (58).

Finally, the NMDA receptor and nNOS may be modulated at different levels in the different subregions by mechanisms that may range from the organization of the NMDA receptor–postsynaptic density-95 protein–nNOS molecular complexes through protein–protein interactions to the action of superoxide anion ($O_2^{\bullet -}$). For instance, PIN, the protein inhibitor of nNOS expressed in the hippocampus, inhibits nNOS by binding to monomers and thus blocking dimerization or even by dissociating already formed dimers (59, 60).

Likewise, $O_2^{\bullet -}$ produced by NMDA receptor activation appears to work in conjunction with $^{\bullet}$NO during induction of LTP in hippocampus (61). It is noteworthy that in rat brain the localization of Cu/Zn-SOD overlaps with that of NOS in the pyramidal cell layers of CA1, CA3, and DG subregions of hippocampus (62). Also, a regional vulnerability to $O_2^{\bullet -}$ has been reported in organotypic hippocampal slice cultures, being CA1 pyramidal neurons selectively affected (63), a pattern of damage similar to that observed after hypoxia/ischaemia (64). Considering the very fast reaction of both superoxide dismutase (SOD) [$K = 2.3 \times 10^9$ $M^{-1}{\cdot}s^{-1}$ (65)] and $^{\bullet}$NO [$K = 1.9 \times 10^{10}$ $M^{-1}{\cdot}s^{-1}$ (66)] with $O_2^{\bullet -}$, the latter yielding cytotoxic peroxynitrite, the production of $O_2^{\bullet -}$ accompanying the synthesis of $^{\bullet}$NO requires fine-tuning between the competition of SOD and $^{\bullet}$NO for $O_2^{\bullet -}$. A disturbance in the balance between the levels of $^{\bullet}$NO and $O_2^{\bullet -}$ would determine differently the availability of $^{\bullet}$NO for transcellular diffusion in hippocampal subregions, which, accordingly, would be reflected in effective $^{\bullet}$NO concentration.

The implications of this study for cell function are as follows: the $^{\bullet}$NO production in the dependency of NMDA receptor activation has been shown to participate in LTP as a retrograde messenger but also in excitotoxic cell death. In the former, $^{\bullet}$NO is assumed to be at low nM concentration, whereas the latter is associated with excessive stimulation of NMDA receptor and, therefore, it is alleged a high production of possibly pathologic $^{\bullet}$NO concentration at the micromolar level. A selective vulnerability of the CA1 subregion to NMDA and glutamate stimuli has been reported (67). In this study, subregions of hippocampus respond differently in terms of $^{\bullet}$NO production. In the CA1 pyramidal cell layer, $^{\bullet}$NO concentration reached the highest levels (typically ≈250 nM) but, even under conditions of continuous NMDA stimulation, $^{\bullet}$NO rose only transiently. Assuming that data obtained with isolated brain slices reflect the concentrations *in vivo*, the claimed high concentration of $^{\bullet}$NO at micromolar range in excitotoxicity achieved by excessive stimulation of NMDA receptor may have to be reevaluated. Moreover, it may have implications for the $^{\bullet}$NO-dependent excitotoxic pathways in the different regions after NMDA receptor activation. Finally, the differential concentration dynamics may reflect distinct regulatory pathways and biological activities for $^{\bullet}$NO in hippocampal subregions.

This work was supported by a grant from Fundação Ciência e Tecnologia and Fundo Europeu de Desenvolvimento Regional Grant POCTI/2001/BCI/42365. G.A.G. was supported by Public Health Service Grants MH01245 and MH58414.

1. Garthwaite, J. & Boulton, C. L. (1995) *Annu. Rev. Physiol.* **57,** 683–706.
2. Prast, H. & Philippu, A. (2001) *Prog. Neurobiol.* **64,** 51–68.
3. Lancaster, J. R., Jr. (1994) *Proc. Natl. Acad. Sci. USA* **91,** 8137–8141.
4. Wood, J. & Garthwaite, J. (1994) *Neuropharmacology* **33,** 1235–1244.
5. Lancaster, J. R., Jr. (1997) *Nitric Oxide* **1,** 18–30.
6. Arancio, O., Lev-Ram, V., Tsien, R. Y., Kandel, E. R. & Hawkins, R. D. (1996) *J. Physiol. (Paris)* **90,** 321–322.
7. Arancio, O., Kiebler, M., Lee, C. J., Lev-Ram, V., Tsien, R. Y., Kandel, E. R. & Hawkins, R. D. (1996) *Cell* **87,** 1025–1035.
8. Arancio, O., Antonova, I., Gambaryan, S., Lohmann, S. M., Wood, J. S., Lawrence, D. S. & Hawkins, R. D. (2001) *J. Neurosci.* **21,** 143–149.
9. Micheva, K. D., Buchanan, J., Holz, R. W. & Smith, S. J. (2003) *Nat. Neurosci.* **6,** 925–932.
10. Jarrard, L. E. (1995) *Behav. Brain Res.* **71,** 1–10.
11. Morrison, J. H. & Hof, P. R. (2002) *Prog. Brain Res.* **136,** 467–486.
12. Brenman, J. E., Chao, D. S., Gee, S. H., McGee, A. W., Craven, S. E., Santillano, D. R., Wu, Z., Huang, F., Xia, H., Peters, M. F., *et al.* (1996) *Cell* **84,** 757–767.
13. Dawson, V. L. & Dawson, T. M. (1998) *Prog. Brain Res.* **118,** 215–229.
14. Cummings, J. A., Nicola, S. M. & Malenka, R. C. (1994) *Neurosci. Lett.* **176,** 110–114.
15. O'Dell, T. J., Hawkins, R. D., Kandel, E. R. & Arancio, O. (1991) *Proc. Natl. Acad. Sci. USA* **88,** 11285–11289.
16. Schuman, E. M. & Madison, D. V. (1991) *Science* **254,** 1503–1506.
17. Coyle, J. T. & Puttfarcken, P. (1993) *Science* **262,** 689–695.
18. Dawson, V. L., Dawson, T. M., London, E. D., Bredt, D. S. & Snyder, S. H. (1991) *Proc. Natl. Acad. Sci. USA* **88,** 6368–6371.
19. Barbosa, R. M., Silva, A. M., Tome, A. R., Stamford, J. A., Santos, R. M. & Rosario, L. M. (1998) *J. Physiol. (London)* **510,** 135–143.
20. Ledo, A., Barbosa, R. M., Frade, J. & Laranjinha, J. (2002) *Methods Enzymol.* **359,** 111–125.
21. Ferreira, N. R., Ledo, A., Frade, J. G., Gerhardt, G. A., Laranjinha, J. & Barbosa, R. M. (2005) *Anal. Chim. Acta* **535,** 1–7.
22. Friedemann, M. N., Robinson, S. W. & Gerhardt, G. A. (1996) *Anal. Chem.* **68,** 2621–2628.
23. Wendland, B., Schweizer, F. E., Ryan, T. A., Nakane, M., Murad, F., Scheller, R. H. & Tsien, R. W. (1994) *Proc. Natl. Acad. Sci. USA* **91,** 2151–2155.
24. Burette, A., Zabel, U., Weinberg, R. J., Schmidt, H. H. & Valtschanoff, J. G. (2002) *J. Neurosci.* **22,** 8961–8970.
25. Jiang, C., Agulian, S. & Haddad, G. G. (1991) *Brain Res.* **568,** 159–164.
26. Lancaster, J. R., Jr. (1996) *Methods Enzymol.* **268,** 31–50.
27. Lewis, R. S. & Deen, W. M. (1994) *Chem. Res. Toxicol.* **7,** 568–574.
28. Liu, K. J., Bacic, G., Hoopes, P. J., Jiang, J., Du, H., Ou, L. C., Dunn, J. F. & Swartz, H. M. (1995) *Brain Res.* **685,** 91–98.
29. Erecinska, M. & Silver, I. A. (2001) *Respir. Physiol.* **128,** 263–276.
30. Mulkey, D. K., Henderson, R. A., 3rd, Olson, J. E., Putnam, R. W. & Dean, J. B. (2001) *J. Appl. Physiol.* **90,** 1887–1899.
31. Cadenas, E. & Packer, L., eds. (2002) *Methods Enzymol.* **359,** 1–514.
32. Taha, Z. (2003) *Talanta* **61,** 3–10.
33. Dinerman, J. L., Dawson, T. M., Schell, M. J., Snowman, A. & Snyder, S. H. (1994) *Proc. Natl. Acad. Sci. USA* **91,** 4214–4218.
34. Kantor, D. B., Lanzrein, M., Stary, S. J., Sandoval, G. M., Smith, W. B., Sullivan, B. M., Davidson, N. & Schuman, E. M. (1996) *Science* **274,** 1744–1748.
35. Topel, I., Stanarius, A. & Wolf, G. (1998) *Brain Res.* **788,** 43–48.
36. Downen, M., Zhao, M. L., Lee, P., Weidenheim, K. M., Dickson, D. W. & Lee, S. C. (1999) *J. Neuropathol. Exp. Neurol.* **58,** 12–21.
37. Blackshaw, S., Eliasson, M. J., Sawa, A., Watkins, C. C., Krug, D., Gupta, A., Arai, T., Ferrante, R. J. & Snyder, S. H. (2003) *Neuroscience* **119,** 979–990.
38. Liu, P., Smith, P. F., Appleton, I., Darlington, C. L. & Bilkey, D. K. (2003) *Neuroscience* **119,** 679–687.
39. Murphy, S., Simmons, M. L., Agullo, L., Garcia, A., Feinstein, D. L., Galea, E., Reis, D. J., Minc-Golomb, D. & Schwartz, J. P. (1993) *Trends Neurosci.* **16,** 323–328.
40. Beckman, J. S. & Koppenol, W. H. (1996) *Am. J. Physiol.* **271,** C1424–C1437.
41. Schuman, E. M. & Madison, D. V. (1994) *Annu. Rev. Neurosci.* **17,** 153–183.
42. Rengasamy, A. & Johns, R. A. (1993) *Mol. Pharmacol.* **44,** 124–128.
43. Griscavage, J. M., Fukuto, J. M., Komori, Y. & Ignarro, L. J. (1994) *J. Biol. Chem.* **269,** 21644–21649.
44. Lei, S. Z., Pan, Z. H., Aggarwal, S. K., Chen, H. S., Hartman, J., Sucher, N. J. & Lipton, S. A. (1992) *Neuron* **8,** 1087–1099.
45. Manzoni, O. & Bockaert, J. (1993) *J. Neurochem.* **61,** 368–370.
46. Lipton, S. A., Choi, Y. B., Pan, Z. H., Lei, S. Z., Chen, H. S., Sucher, N. J., Loscalzo, J., Singel, D. J. & Stamler, J. S. (1993) *Nature* **364,** 626–632.
47. Stamler, J. S., Toone, E. J., Lipton, S. A. & Sucher, N. J. (1997) *Neuron* **18,** 691–696.
48. Fagni, L., Livier, M., Lafon-Cazal, M. & Bockaert, J. (1995) *Mol. Pharmacol.* **47,** 1239–12347.
49. Choi, Y. B., Tenneti, L., Le, D. A., Ortiz, J., Bai, G., Chen, H. S. & Lipton, S. A. (2000) *Nat. Neurosci.* **3,** 15–21.
50. Griffiths, C. & Garthwaite, J. (2001) *J. Physiol. (London)* **536,** 855–862.
51. Griffiths, C., Yamini, B., Hall, C. & Garthwaite, J. (2002) *Biochem. J.* **362,** 459–464.
52. Bredt, D. S. & Snyder, S. H. (1990) *Proc. Natl. Acad. Sci. USA* **87,** 682–685.
53. Bliss, T. V. & Collingridge, G. L. (1993) *Nature* **361,** 31–39.
54. Nicoll, R. A. & Malenka, R. C. (1995) *Nature* **377,** 115–118.
55. West, G. J., Kawas, C. H., Martin, L. J. & Troncoso, J. C. (2000) *Ann. N.Y. Acad. Sci.* **908,** 255–259.
56. Thompson, C. L., Drewery, D. L., Atkins, H. D., Stephenson, F. A. & Chazot, P. L. (2002) *Brain Res. Mol. Brain Res.* **102,** 55–61.
57. Smith, D. A., Hoffman, A. F., David, D. J., Adams, C. E. & Gerhardt, G. A. (1998) *Neurosci. Lett.* **255,** 127–130.
58. Kojima, H., Hirotani, M., Nakatsubo, N., Kikuchi, K., Urano, Y., Higuchi, T., Hirata, Y. & Nagano, T. (2001) *Anal. Chem.* **73,** 1967–1973.
59. Greenwood, M. T., Guo, Y., Kumar, U., Beausejours, S. & Hussain, S. N. (1997) *Biochem. Biophys. Res. Commun.* **238,** 617–621.
60. Jaffrey, S. R. & Snyder, S. H. (1996) *Science* **274,** 774–777.
61. Klann, E., Roberson, E. D., Knapp, L. T. & Sweatt, J. D. (1998) *J. Biol. Chem.* **273,** 4516–4522.
62. Okabe, M., Saito, S., Saito, T., Ito, K., Kimura, S., Niioka, T. & Kurasaki, M. (1998) *Free Radical Biol. Med.* **24,** 1470–1476.
63. Wilde, G. J., Pringle, A. K., Wright, P. & Iannotti, F. (1997) *J. Neurochem.* **69,** 883–886.
64. Pringle, A. K., Iannotti, F., Wilde, G. J., Chad, J. E., Seeley, P. J. & Sundstrom, L. E. (1997) *Brain Res.* **755,** 36–46.
65. Fridovich, I. (1995) *Annu. Rev. Biochem.* **64,** 97–112.
66. Kissner, R., Nauser, T., Bugnon, P., Lye, P. G. & Koppenol, W. H. (1997) *Chem. Res. Toxicol.* **10,** 1285–1292.
67. Vornov, J. J., Tasker, R. C. & Coyle, J. T. (1991) *Exp. Neurol.* **114,** 11–22.